Iranian Journal of Science and Technology, Transactions of Mechanical Engineering (2021) 45:1071–1090
https://doi.org/10.1007/s40997-020-00366-5

RESEARCH PAPER

Effect of Distributed Damping on the Dynamic Behavior of Flexible Chassis of Heavy Road Vehicle Under Standardized Random Road Responses

Ashish Gupta[1] · **Vikas Rastogi**[2]

Received: 22 April 2019 / Accepted: 23 May 2020 / Published online: 23 June 2020

Abstract
This paper evaluates the dynamics of a heavy road truck on different random road conditions, whereas the issue of beam flexibility is also being accompanied. Heavy vehicles like trucks and buses having a large structure to carry their load ride in all kinds of terrains, for thousands of miles without failing structure. Structure (chassis or frame) of the truck should be able to sustain all types of vibration (i.e., longitudinal, transverse and flexural). This study starts with developing an analytical model with consideration of the Rayleigh beam approach, where the rotary inertia of the beam has also been admitted. This work also considered internal damping of the chassis, which has been neglected in past studies specifically for flexural vibration. Further bond graph model of the flexible structure of a heavy road vehicle is developed, where this model is derived through modal expansion approach. The dynamic response of the structure is analyzed under various random road conditions at different vehicle speeds. These random models of the road are developed according to ISO 8608 standard, whereas four (H1–H4) kinds of road categories are considered. Results show the dynamic response of the chassis under a real road response so that parameters of the various parts of the structure can be evaluated, which further raises the ride comfort and road holding capability of the structure. Further, this work also examines the effect of structural damping or internal damping on the dynamics of the system.

Keywords Lagrangian approach · Bond graph · Frame flexibility of the chassis · Structural damping · Random road conditions

1 Introduction

Ride vibration is a principal concern for vehicle dynamics, where frame flexibility plays a very significant role. Numerous studies have been conducted on problems of ride vibration. However, very few studies have been carried out to study the effect of vibration, which includes a flexible frame. It has been generally noticed that the flexural vibration can be neglected for smaller vehicles, relatively for stiffer automobiles. However, trucks and the long heavy vehicle experience significant beaming mode vibration (Margolis and Edeal 1989). Ibrahim (1996) has created a model of truck frame through FEM where he calculated the modal properties of the frame. The results were presented in terms of PSD and RMS of the vehicle vertical response. Most of the analyses on the effects of chassis flexibility in vehicle dynamics were based on the use of particular model developed, whereas the FEM (finite element method) and the modal superposition theory have been extensively used to calculate the modal properties of the frame structure. Generally, the problem occurs due to the beam flexibility of the vehicle, which is termed as 'beaming response of the vehicle' (Rideout 2012). Rideout and Khan (2010) presented the model of the frame flexibility issue for truck model. They created a pitch plane model which involved longitudinal dynamics and transverse frame vibrations. Huang and Zeng (2010) studied about flexural vibration problems for high-speed passenger rail vehicle, where car body was modeled through Euler beam approach. This research underlined

✉ Ashish Gupta
ashish.gupta@glbitm.ac.in; ashish.j001@gmail.com

[1] Mechanical Engineering Department, G.L Bajaj Institute of Technology and Management, Greater Noida 201306, India

[2] Design Centre, Department of Mechanical Engineering, Delhi Technological University, Delhi 110042, India

the effect of internal damping in ride comfort of rail vehicle. Kumar et al. (2017) analyzed the whole-body vibration for railway system. They have considered biodynamic model of human for the assessment of ride comfort, where whole-body model was integrated with flexible bogie model system. The flexible bogie system was modeled through Euler–Bernoulli beam approach. Similarly in other studies, Euler–Bernoulli approach was attempted to introduce beam flexibility in heavy truck chassis modeling (Zhou et al. 2009; Kim and Yim 1994). Heavy long vehicles have a ladder-type chassis structure across the whole length of the vehicle. These structures are stiffer in bending, which can respond to bending frequencies more than 20 Hz. When the engine and other elements are mounted on the structure, these bending frequencies are reduced up to 8 Hz, for highly stiffer frames (Cai-hong and Zeng 2010; Tomioka et al. 2017). Tomioko and Takigami (2015) have conducted the experimental study on flexural beam to evaluate the effect of frame flexibility on passenger comfort. Some other studies apparently show that the beaming frequency is higher than the rigid frequency of the vehicle (Tomioka et al. 2006; Agostinacchio et al. 2014). However, in large vehicles, beaming frequency is influenced by road inputs.

A lot of research has been conducted considering the issue of frame flexibility in the analysis of railway vehicle. But, limited studies were reported on dynamic analysis of heavy road vehicles considering random road disturbances. A country like India, where multifarious road conditions are present, which creates an infirm condition before all leading automobile industries to maintain comfort level as per standard on every road conditions. Some studies have mentioned that structural damping can participate in ride quality improvement. So, in the present work frame flexibility has been incorporated by considering frame as Raleigh beam, which also includes the effect of the rotary inertia. Lagrangian approach has been applied to obtain the energy equations for the vehicle system, which resulted from the well-known rigid body modes and the modal parameters of the frame flexibility. The work involves the importance of structural or internal damping of beam-type chassis structure on flexural vibration and ride quality of the heavy vehicle with random road disturbance prescribed by ISO 8608 (Meirovitch 1980) as input. The bond graph approach has been utilized to model the vehicle with flexible frame. Besides the beam response, the effect of different road conditions as per ISO 8608 and vehicle speeds on the dynamics of vehicle has also been presented. The work begins with deriving Lagrange equation of frame considered as Rayleigh beam for truck flexural response. Then, this formulation is being extended for bond graph modeling with or without consideration of structural damping effect. Simulations were carried out to visualize the beaming mode response with respect to random road conditions as prescribed by ISO 8608.

2 Analytical Framework for Heavy Vehicle System Through Classical Mechanics

2.1 Generalized Lagrange's Equation for a Continuous System

It is a well-known fact that the Lagrange formulation provides one of the most convenient ways of writing down the equation of motion for a wide range of mechanical systems. The principal advantage of Lagrange's equation is that it is easier to apply to dynamical systems other than the simplest. This formulation is created from scalar quantities of kinetic energy, potential energy and work expressed in terms of generalized coordinates and developed for universal handling of dynamical systems (Mukherjee and Karmakar 2000). The equation is formulated equations of motion from the principle of least action. This density function is a function comprised of time, transverse displacements and transverse velocities, and up to second derivatives of displacements to space coordinates x, which may be expressed as

$$\widehat{L}\big(w(t,x),\dot{w}(t,x),w'(t,x),w''(t,x),\dot{w}'(t,x)\big)=\hat{T}(t,x)-\hat{V}(t,x) \tag{1}$$

where $\widehat{L}(\cdot)$ is the Lagrangian density function and $\hat{T}(\cdot)$ is the kinetic energy density, which may be expressed as,

$$\widehat{T}(x,t)=\widehat{T}(\dot{w}(x,t),\dot{w}'(x,t)) \tag{2}$$

Moreover, $\hat{V}(t,x)$ is the potential energy density, which has the following functional dependence,

$$\widehat{V}(x,t)=\widehat{V}(w'(x,t),w''(x,t)) \tag{3}$$

The next step is used for finding the equation of motion and the boundary conditions for the beam through the variational principle (see Appendix 2). This formulation yields

$$\delta\int_{t1}^{t2}\widehat{L}\big(w(t,x),\dot{w}(t,x),w'(t,x),w''(t,x),\dot{w}'(t,x)\big)\mathrm{d}t=0 \tag{4}$$

where $\delta(\cdot)$ is infinitesimal variation operator and it is very similar to the total derivative operator; the only difference is that $\delta(\cdot)$ does not vary with time. Another significant property of infinitesimal operator is that it commutes with the differential operator. Using the extremization condition, one may obtain

$$\int_0^L\int_{t1}^{t2}\delta\widehat{L}\big(w(t,x),\dot{w}(t,x),w'(t,x),w''(t,x),\dot{w}'(t,x)\big)\,\mathrm{d}x\mathrm{d}t=0 \tag{5}$$

or

$$\int_0^L \int_{t1}^{t2} \left[\frac{\partial \widehat{L}}{\partial w}\delta w + \frac{\partial \widehat{L}}{\partial \dot{w}}\delta \dot{w} + \frac{\partial \widehat{L}}{\partial w'}\delta w' + \frac{\partial \widehat{L}}{\partial \dot{w}'}\delta \dot{w}' + \frac{\partial \widehat{L}}{\partial w''}\delta w'' \right] \mathrm{d}x\,\mathrm{d}t = 0 \tag{6}$$

The detailed derivation of the variational formulation is presented in "Appendix 1."

2.2 Analytical Formulation for Flexural Behavior of the Truck Chassis Structure

An analytical formulation for flexural behavior of the truck structure is being attempted in this section. The vehicle base is modeled as a rigid body with a local coordinate reference frame (w, x) attached to the center of mass (M) and aligned with the inertia principal axes as shown in Fig. 1. It has density (ρ) and $p$itch inertia (J) with respect to the body $W_1(t) - W_2(t)$ displacement axis, EI flexural rigidity and $\theta(t)$ pitch velocity of the base. It is connected with the suspension system to different elements of the vehicles. The spring stiffness characterizes the spring and damper in the suspension system k_s and damping coefficient R_s, respectively. The various displacements of the vehicle are described $w(x, t)$ with respect to the equilibrium positions. As the vehicle is assumed to be rigid, its motion can be described by the vertical displacement (bounce) as $w(x, t)$ and the rotation about the transverse horizontal axis (pitch) as $\dot{\theta}(t)$.

The model of the vehicle is being created with the following assumptions:

- The components of the vehicle body act as a rigid body.
- The springs and dampers of the suspension system have linear characteristics.
- The spring damper system is assumed to be massless.
- The tire is assumed to provide stiffness and thus modeled as a spring element.
- The positions of the two ends of the spring connecting two rigid bodies or connecting one rigid body and one contact point are required as input data.
- The spring damper system connects each rigid body.
- The traveling road is assumed to be straight.
- The road inputs are assumed to be random.

The analytical framework of truck chassis can be assumed as a free–free beam structure, where Rayleigh beam approach is being adopted. Let us consider a transverse deflection of the beam $w(x,t)$, where x varies from 0 to beam length L. The formalism of beam flexibility is easily obtained through the well-known Lagrangian equation. Lagrangian density variation may be obtained from the following expression as

$$L = \left[\frac{1}{2}\int_0^L \left(\rho A \dot{w}(x,t)^2 + \rho I \dot{w}'(x,t)^2\right)\mathrm{d}x - \frac{1}{2}\int_0^L \left(EIw''(x,t)^2\right)\mathrm{d}x \right] \tag{7}$$

where ρ is the mass density, A is the area of cross section, EI is the rigidity and I is the second moment of area of the cross section of the beam about the neutral axis. In Eq. (7), the first term represents kinetic energy of the beam, the second term presents as inertial energy and the final term is strain energy. The variational formulation presents a refined and classical method of deriving the equation of motion of a dynamical system, where all the boundary conditions of a system can be revealed. However, fundamentals of variational formulation for the continuous system are detailed in "Appendix 2."

The equation of motion is obtained after applying a variational formulation and boundary conditions in free vibration condition, which may be expressed as

$$\rho A \ddot{w}(x,t) - \left(\rho I \dot{w}''(x,t)\right)' + \left(EIw''(x,t)\right)'' = 0 \tag{8}$$

This equation of motion is based on Rayleigh beam model. The term $\left(EIw''(x,t)\right)''$ is usually referred to as the

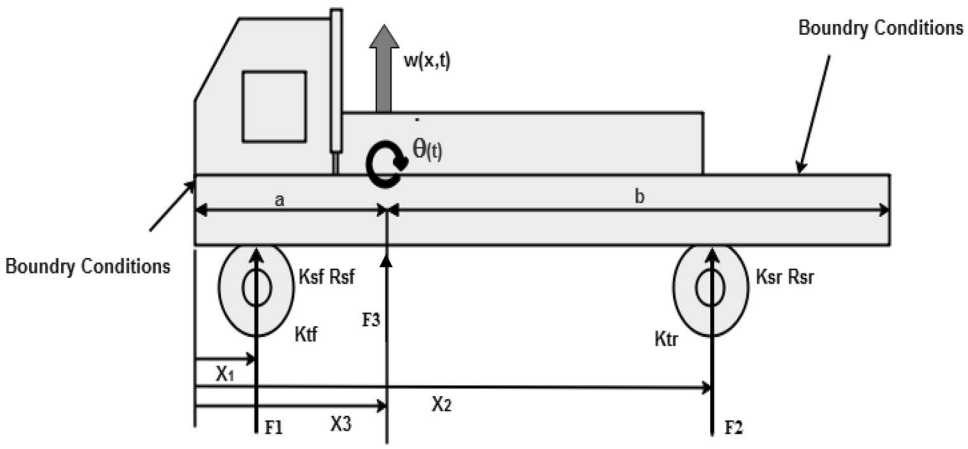

Fig. 1 Schematic diagram of a continuous frame of vehicle

flexural term, where EI is called the flexural stiffness and $\left(\rho I\dot{w}''(x,t)\right)'$ is known as the rotary inertia term. If this term is zero, then Eq. (8) will become a Euler beam model. Thus, the term $\left(\rho I\dot{w}''(x,t)\right)'$ can also be named as a Rayleigh beam term.

Assume a modal solution for Eq. (8) in the form of

$$w(x,t) = W(x)e^{i\omega t} \tag{9}$$

where ω is the eigenfrequency and $W(x)$ is the eigenfunction. The actual solution of the equation may be obtained by taking the real part of the solution. Substituting the modal solution in the field Eq. (8) yields after rearrangement as

$$-\omega^2\left[\rho AW - \left(\rho IW'\right)'\right] + \left(EIW''\right)'' = 0 \tag{10}$$

which along with the corresponding boundary condition represents the eigenvalue problem for a Rayleigh beam.

2.3 Modal Analysis for Uniform Rayleigh Beam

Considering Eq. (10) as a uniform beam and substituting in Eq. (9) a solution of the form

$$W(x) = Ce^{\lambda x} \tag{11}$$

where C and λ are constants, Eq. (10) can be rewritten as

$$EI\lambda^4 - \omega^2\rho I\lambda^2 - \omega^2\rho A = 0 \tag{12}$$

yielding

$$\lambda^2 = \frac{1}{2EI}\left[\omega^2\rho I \pm \sqrt{\omega^4\rho^2I^2 + 4\omega^2EI\rho A}\right]$$

Thus, the spatial equation (real form) of Eq. (12) has the general solution, which may be expressed as

$$W(x) = A\cosh\lambda x + B\sinh\lambda x + C\cos\lambda x + D\sin\lambda x \tag{13}$$

Here, one may consider a uniform Rayleigh beam for which the free–free boundary conditions are given by

$$W(0) = 0, \quad W'(0) = 0, \quad W''(l) = 0, \quad W'''(l) = 0, \tag{14}$$

Using, Eq. (14) in Eq. (13) yields the frequency equation as

$$\cosh\lambda_n l\cos\lambda_n l - 1 = 0 \tag{15}$$

The solution of Eq. (15) yields

$$\lambda_n = \left(\frac{2n+1}{2}\pi\right)\frac{1}{l}$$

Moreover, the mode shape function may be expressed as

$$\begin{aligned} W_n(x) = {} & (\cos\lambda_n l - \cosh\lambda_n l)(\sin\lambda_n x + \sinh\lambda_n x) \\ & - (\sin\lambda_n l - \sinh\lambda_n l)(\cos\lambda_n x + \cosh\lambda_n x) \end{aligned} \tag{16}$$

Thus, one may obtain the natural frequency of Eq. (6), which may be written as

$$\omega_n = \lambda_n^2\frac{1}{\left[1+\lambda_n^2\frac{I}{A}\right]^{1/2}}\sqrt{\frac{EI}{\rho A}} \tag{17}$$

It is recognized that conditions are force-free at this point, which permits $\omega_n = 0$ to be a mode frequency. Thus, Eq. (10) will be written as

$$\frac{\mathrm{d}^4W}{\mathrm{d}x^4} = 0 \tag{18}$$

or

$$W = c_1x^3 + c_2x^2 + c_1x + c_4 \tag{19}$$

There are two possible solutions for Eq. (13), which satisfied all boundary conditions. They are $W = \text{const}$ and $W = ax + b$. These are called rigid body modes, and it is convenient to assume them as rigid body rotation of the beam about the centrally located center of mass. Thus,

$$W_{00}(x) = 1 \tag{20}$$

and

$$W_0(x) = x - \frac{L}{2} \tag{21}$$

Let us consider an analysis for truck chassis, which is presented in Fig. 1. In this figure, the half model of the road truck is supported by front and rear suspension, which exerted an external force on the beam over the various road responses. From equation of motion, Eq. (8) will be rewritten as

$$\begin{aligned} & \rho A\ddot{w}(x,t) - \left(\rho I\dot{w}''(x,t)\right)' + \left(EIw''(x,t)\right)'' \\ & = F_1\delta(x-x_1) + F_2\delta(x-x_2) + F_3\delta(x-x_3) \end{aligned} \tag{22}$$

where F_1 and F_2 are the force exerted by front and rear suspension systems, respectively, and F_3 is dead weight on the beam, $\delta(\cdot)$ is the Dirac delta function, x_1 and x_2 are the respective distance from left end to the front and rear suspension of the vehicle, respectively, and x_3 is the distance of dead weight from the left end. One may assume that the solution of Eq. (22) is separable in space and time, and the forced solution has the following form,

$$w(x,t) = \sum_{n=0}^{\infty} W_n(x)U_n(t) \tag{23}$$

where $W_n(x)$ depends on the spatial position and $U_n(t)$ depends on time. Introducing Eq. (23) into Eq. (22), and multiplying each term by $W_m(x)$ and integrating with respect

to $x=0$, $x=l$, one may then use the orthogonal property to the modes and obtain

$$\int_0^l \rho A W_n^2 \mathrm{d}x\ddot{U}(t) + \omega_n^2(\rho I\lambda_n^2 - \rho A)\int_0^l W_n^2 \mathrm{d}xU(t) = F_1 W_n(x_1) + F_2 W_n(x_2) + F_3 W_n(x_3) \tag{24}$$

$$\rho A\left(1 - \frac{I}{A}\lambda_n^2\right)\int_0^l W_n^2 \mathrm{d}x\ddot{U}(t) + \rho A\left(1 - \frac{I}{A}\lambda_n^2\right)\omega_n^2\int_0^l W_n^2 \mathrm{d}xU(t) = F_1 W_n(x_1) + F_2 W_n(x_2) + F_3 W_n(x_3) \tag{25}$$

Equation (25) can be represented in general form as

$$m\ddot{U}(t) + kU(t) = F_1 W_n(x_1) + F_2 W_n(x_2) + F_3 W_n(x_3) \tag{26}$$

where

$$m = \rho A\left(1 - \frac{I}{A}\lambda_n^2\right)\int_0^l W_n^2 \mathrm{d}x$$

$$k = m\omega_n^2\int_0^l W_n^2 \mathrm{d}x$$

Now one may write the first frequency modes (Karnopp et al. 2012)

$$\left[\rho A\int_0^l (1)_n^2 \mathrm{d}x\right]\ddot{U}_{00} = F_1 + F_2 + F_3 \quad \text{or} \quad m\ddot{U}_{00} = F_1 + F_2 + F_3 \tag{27}$$

which states that the external force accelerates the center of mass of the beam. The other zero frequency mode yields

$$\left[\rho A\int_0^l \left(x - \frac{l}{2}\right)^2 \mathrm{d}x\right]\ddot{U}_{00} = F_1 + F_2 + F_3 \tag{28}$$

or

$$J\ddot{U}_0 = F_1 + F_2 + F_3$$

This equation states that the moment of the external forces about the center of mass produces angular acceleration $\ddot{U}_{00}$, where J is the centroid moment of inertia of beam. The next subsection will present the formulation, which includes structural damping.

2.4 Incorporation of Structural Damping

Now one may consider internal damping (the detailed derivation of internal damping is presented in "Appendix 2" for ready reference) of the beam and Eq. (22) may be rewritten as

$$\rho A\ddot{w}(x,t) - \left(\rho I\dot{w}''(x,t)\right)' + \left(EIw''(x,t)\right)'' - \mu_I I\left(\dot{w}'''\right)' = F_1\delta(x - x_1) + F_2\delta(x - x_2) + F_3\delta(x - x_3) \tag{29}$$

$$\rho A\ddot{w}(x,t) - \left(\rho I\dot{w}''(x,t)\right)' + \omega^2(\rho I\lambda^2 - \rho A) - \mu_I I\left(\dot{w}'''\right)' = F_1\delta(x - x_1) + F_2\delta(x - x_2) + F_3\delta(x - x_3) \tag{30}$$

where μ_I is the structural damping coefficient, δ is the Dirac delta function, x_1 and x_2 are the respective distance from left corner to the front and rear suspension of the vehicle and x_3 is the distance of dead weight from the extreme left corner of the vehicle. F_1 and F_2 are the suspension forces of the front and rear suspension system, respectively, and F_3 is the dead weight. The front and rear suspension forces of the vehicle may be expressed as

$$F_1 = C_\mathrm{s}^\mathrm{f}(V_\mathrm{f} - \dot{w}_1) + K_\mathrm{s}^\mathrm{f}\left(\int_0^t V_\mathrm{f}\mathrm{d}t - w_1\right) \tag{31}$$

$$F_2 = C_\mathrm{s}^\mathrm{r}(V_\mathrm{r} - \dot{w}_2) + K_\mathrm{s}^\mathrm{r}\left(\int_0^t V_\mathrm{r}\mathrm{d}t - w_2\right) \tag{32}$$

where C_s^f and C_s^r are, respectively, damping coefficient of the front and rear damper; V_f and V_r are the road velocity input at front and rear wheel, respectively; K_s^f and K_s^r are the suspension stiffness of front and rear suspension system, respectively; $\dot{w}_1$ and w_1 are the velocity and displacement of front sprung mass; and $\dot{w}_2$ and w_2 are the velocity and displacement of rear sprung mass.

One may assume solution similar to Eq. (24); applying Eqs. (23)–(30), one may obtain a solution as

$$\int_0^l \rho A W_n^2 \mathrm{d}x\ddot{U}(t) + \omega_n^2(\rho I\lambda_n^2 - \rho A)\int_0^l W_n^2 \mathrm{d}xU(t) - \rho I\lambda_n^2\int_0^l W_n^2 \mathrm{d}x\ddot{U}(t) - \mu_I I\lambda_n^4\int_0^l W_n^2 \mathrm{d}x\dot{U}(t) = F_1 W_n(x_1) + F_2 W_n(x_2) + F_3 W_n(x_3) \tag{33}$$

Rearranging Eq. (33), one may obtain

$$\rho A\left(1 - \frac{I}{A}\lambda_n^2\right)\int_0^l W_n^2 \mathrm{d}x\ddot{U}(t) + \rho A\left(1 - \frac{I}{A}\lambda_n^2\right)\omega_n^2\int_0^l W_n^2 \mathrm{d}xU(t) - \mu_I I\lambda_n^4\int_0^l W_n^2 \mathrm{d}x\dot{U}(t) = F_1 W_n(x_1) + F_2 W_n(x_2) + F_3 W_n(x_3) \tag{34}$$

Finally, Eq. (34) may be represented as

$$m_n\ddot{U}(t) + R_n\dot{U}(t) + k_nU(t) = F_1W_n(x_1) + F_2W_n(x_2) + F_3W_n(x_3) \tag{35}$$

where

$$m_n = \rho A\left(1 - \frac{I}{A}\lambda_n^2\right)\int_0^l W_n^2\mathrm{d}x, \tag{36}$$

$$k_n = m\omega_n^2\int_0^l W_n^2\mathrm{d}x, \tag{37}$$

$$R_n = \mu_I I\lambda_n^4\int_0^l W_n^2\mathrm{d}x \tag{38}$$

Equations (36–38) show that the rotary inertia affects the dynamics of the beam, which is not being taken in case of Euler beam. However, in this case, the value of $I/A \cdot \lambda_n^2$ is always less than 1. Generally, distributed elements that one may obtain to involve in almost all the system models are lightly damped. The location of structure damping cannot be precisely identified from where it arises. The mechanism of energy dissipation is very typical and complicated; some dissipation takes place because of the plastic deformation and some of the energy radiation from material surfaces. It is not assured in the modeling that individual conventional damper will attach to model for representing the damping of distributed elements. It can happen if the damping includes functionally by incorporating it into individual modes. This is accompanied by merely appending R-elements to the mode oscillators of the modal bond graph. R-element is represented in Eq. (30), where μ_I is varied from 0.01 to 0.1. The next subsection will present the bond graph modeling to visualize the simulation for different parameters.

3 Bond Graph Modeling of the Truck Chassis Structure

The physical system of a truck chassis (pitch plane model) with front and rear suspension system driven over the random road is presented in Fig. 1. The boundary condition of the structure is taken as free–free. The dynamic disturbance in vertical direction of the vehicle due to random road conditions is the main attraction of this modeling. The longitudinal and lateral dynamics are not considered in the modeling. The bond graph technique is being used as a modeling tool, and the bond graph of the system is created through formulation, which was developed in the previous section. Figure 2 presents the bond graph model of a flexible infinitesimal beam, whereas Fig. 3 shows the bond graph model of a flexible beam with internal damping along with suspension system. The rigid body modes appear simply as inertia elements with associated modal stiffness and damping. The first inertia parameter is the beam mass (M), and second is the beam moment of inertia (Jg). The transformer (-TF-) elements are connected to the rigid body modes, which correctly apply the forces and moments to these elements. The modal masses are taken from Eq. (36), whereas modal stiffness and modal damping can be taken from Eqs. (37) and (38), respectively.

The system is entirely flexible in transverse and bending, but torsionally rigid. Each 0-junction is attached to each 1-junction with modal components through transformer (TF) elements with moduli equal to appropriate mode function. The transformer function is moduli with shape function (W_n), and the values of this function can be determined from Eq. (16). The attached systems are then appropriately appended to the external 0-junction bonds to form a complete, low-order, very accurate model. Figure 3 shows a general finite mode representation with two input (front and rear) location, where Eq. (26) represents a governing contribution of ith mode.

In the real world, distributed elements have some damping properties, which resist vibration level up to a certain level. No mechanism can quickly identify the value of damping on specific. However, only the quantity of dissipative energy can be determined. It is customary not to attempt to perform detailed modeling of the damping mechanism, but instead to include damping functionally by incorporating its individual modes. This is accomplished by simply appending R-elements to the mode oscillator of the bond graph. The bond graph model of the distributed system including damping modes is presented in Fig. 3. The governing equation of this configuration is mentioned in Eq. (23).

4 Numerical Simulation

Computer simulation can compress the performance of a system over the years into a few minutes of the computer running time. The parameters used for simulation for truck chassis system are presented in Table 1. Simulation models are relatively flexible and can be modified to accommodate the changing environment to the real situation. At present, most of the simulation models are made using differential equations. In this research, a half car flexible model with suspension systems is investigated at

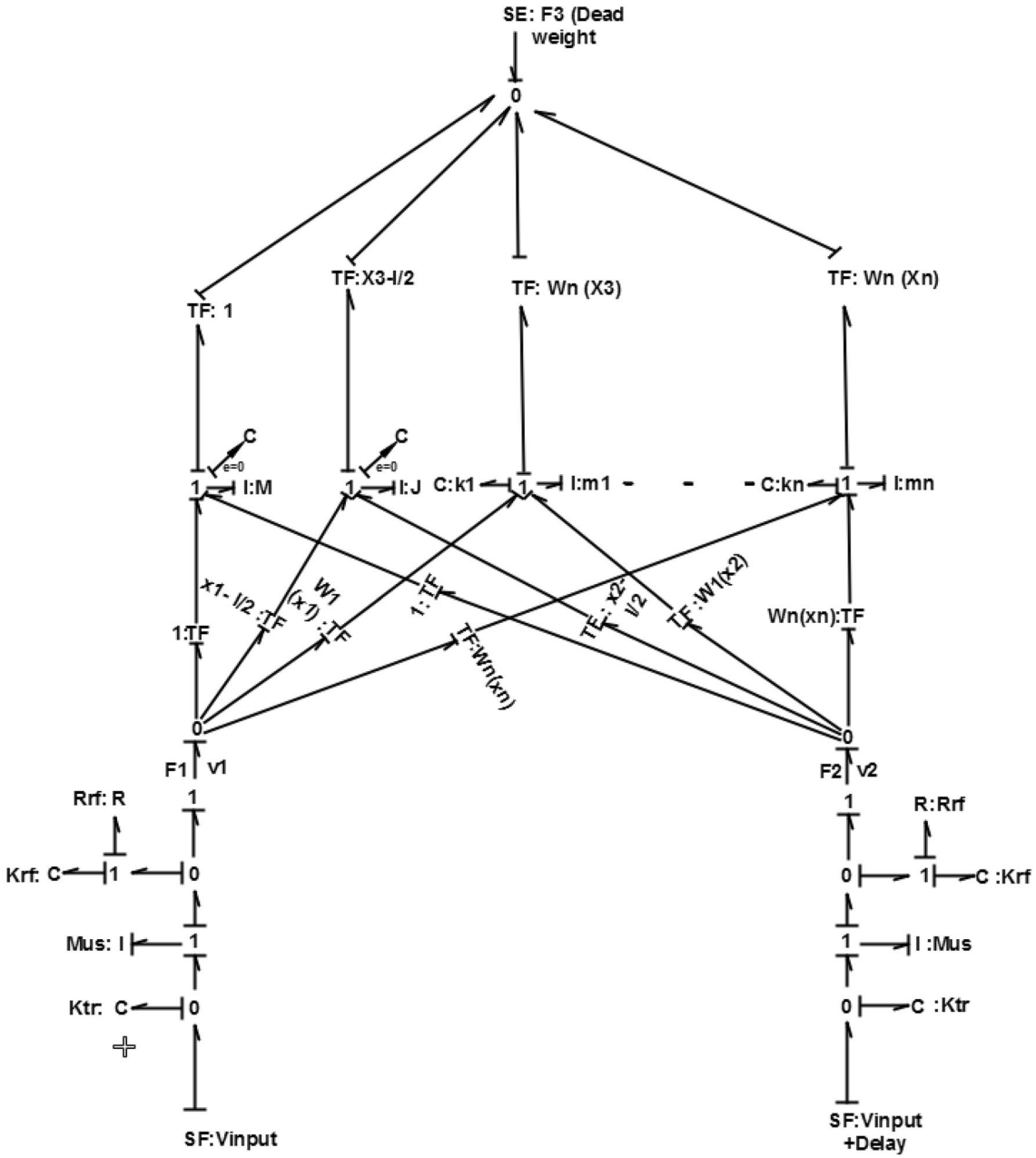

Fig. 2 Bond graph model of truck chassis considering internal damping

different operating speeds on different road profile inputs using bond graph technique and simulators of SYMBOLS Sonata® and MATLAB/Simulink® software are used (Gupta and Rastogi 2016; Hassani 2013; Mukherjee and Samantaray 2006). The bond graph model of the vehicle is simulated for 10 s to obtain different output responses. In total, 1024 records are used in the simulation and error is kept in the order of 5.0×10^{-4}. Fifth-order Runge–Kutta Gill method is used in this present work to solve the various differential equations generated through bond graph model.

4.1 Road Inputs

Two types of road profile inputs of the simulation of this system are used, viz. steady-state input and random road input.

4.1.1 Sine Wave Input

The steady-state input has been taken in a sinusoidal form, and the following expression is used for simulation (Hagedorn and DasGupta 2007):

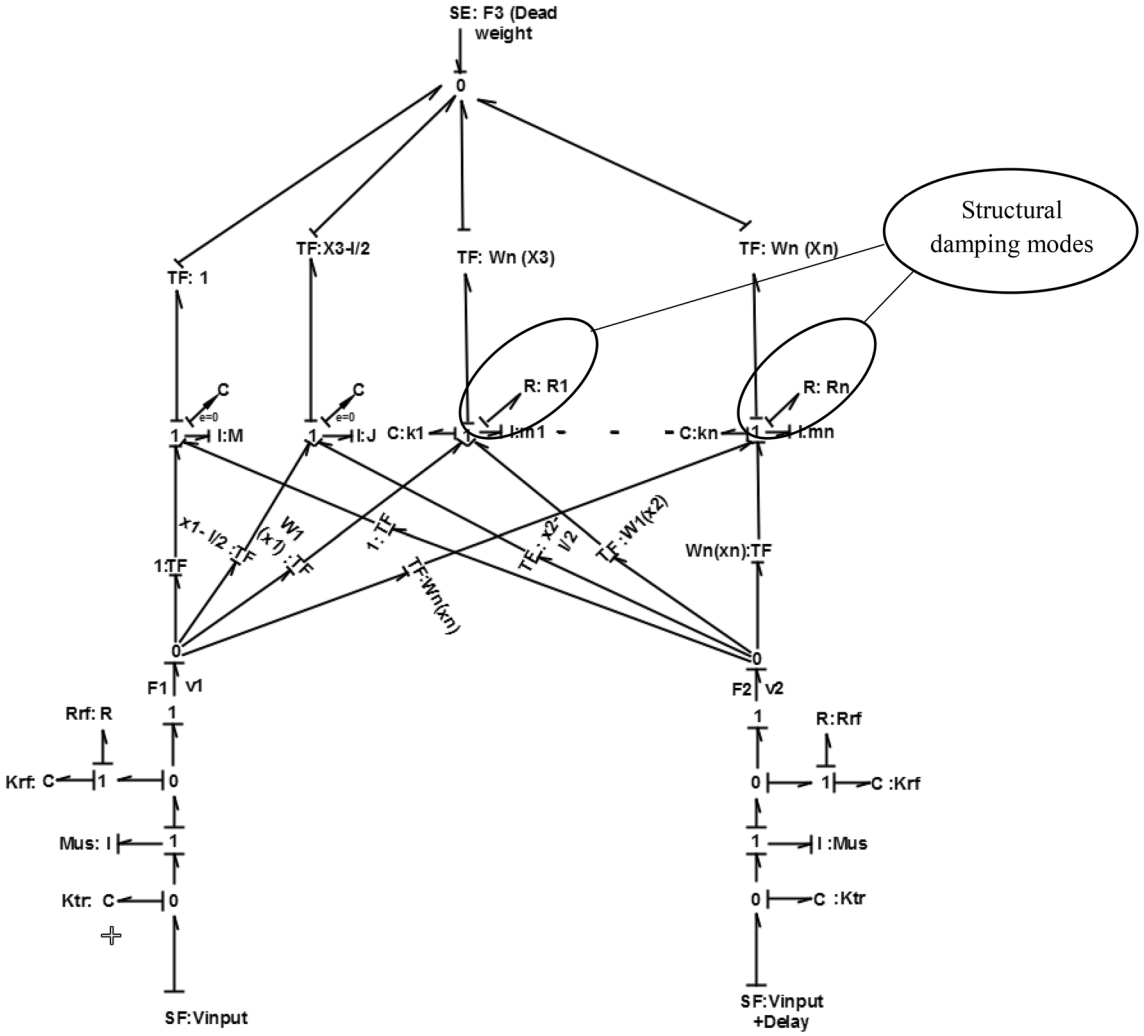

Fig. 3 Bond graph model of truck chassis considering internal damping

Table 1 Simulation parameters for flexible chassis system (Rideout and Khan 2010)

Parameter	Value	Unit
Vehicle length	10	m
Frame mass (Mg)	4350	kg/m
Frame inertia (J)	24,000	kg/m^2
Suspension stiffness (K_{sf}, K_{sr})	375, 870	kN/m
Suspension damping (R_{sf}, R_{sr})	31,895, 33,384	Ns/m
Flexural rigidity (EI)	1.05e+08	N m^2
Unsprung mass (Mus)	50	kg
x_1, x_2, x_3, x_4	2.95, 5.75, 7, 3	m

$$V_{\text{input}} = A_{\text{jump}} * \omega * \sin(\omega * t), \quad \text{for front wheel} \tag{39}$$

$$V_{\text{input}} = A_{\text{jump}} * \omega * \sin(\omega * (t + d/v)), \quad \text{for rear wheel} \tag{40}$$

where A_{jump} is the amplitude of vibration and ω is the excitation frequency.

4.1.2 Random Road Condition

A random road profile is generated according to the International Organization for Standardization (ISO 8608). It gives a depiction of the road profile through estimation of the PSD of the vertical displacements G_d, as a function of spatial frequency $n(n = \Omega/2\pi(\text{cycles})/\text{m})$ and also of angular spatial frequency Ω. ISO 8608 introduces a classification, which is evaluated in accordance with conventional values of spatial frequency $n_0 = 0.1$ cycles/m and angular spatial frequency $\Omega_0 = 1$ cycles/m. There are eight classes of roads mainly

identified from classes H1 to H8 according to the values of $G_d(n)$ and $G_d(\Omega)$ established in ISO 8608, which are shown in Table 2 (Meirovitch 1980).

In the simulation, ISO 8608 provides the roughness of the road surface profile, which may be stated using the following equations:

$$G_d(n) = G_d(n_0)\left(\frac{n}{n_0}\right)^{-w} \tag{41}$$

$$G_d(\Omega) = G_d(\Omega_0)\left(\frac{n}{n_0}\right)^{-w} \tag{42}$$

where w denotes the waviness and its value is taken to be 2 in this case. In this research, random road inputs have been developed by taking into consideration the PSD of vertical displacement G_d as a function of spatial frequency n.

Beginning with a distributed road profile to specify the value of spatial frequency n, looped within a frequency band Δn, the PSD function value is represented through the following expression as

$$G_d(n) = \lim_{\Delta n \to 0}\left(\frac{\psi_x^2}{\Delta n}\right) \tag{43}$$

where the mean square value is denoted by ψ_x^2 which signifies the component of the signal for spatial frequency n contained by the frequency band Δn. Accordingly, the signal of road profile is discretized, and thus, it is characterized by a series of elevation points along with evenly spaced ones. Here, road profile length is denoted by L, whereas the sampling interval is denoted by B. Further, the maximum value of sampling spatial frequency c is $1/B$, the maximum effective sampling spatial frequency (n_{eff}) is $n_{max}/2$ and the discretized spatial frequency values n_i are equally spaced under the frequency domain, with an interval of (Δn) as $1/L$.

So herein, generic spatial frequency value n_i can be regarded as $i{\cdot}\Delta n$ and Eq. (43) may be written in the discrete form as

$$G_d(n) = \frac{\psi_x^2(n_i, \Delta n)}{\Delta n} = \frac{\psi_x^2(i \cdot \Delta n, \Delta n)}{\Delta n} \tag{44}$$

where i varying from 0 to N as $\frac{^n\max}{\Delta n}$, one may obtain the road profile by a simple harmonic function

$$h(x) = A_i \cos(2\pi \cdot n_i \cdot x + \phi) = A_i \cos(2\pi \cdot i \cdot x \cdot \Delta n + \phi) \tag{45}$$

where the amplitude is denoted by A_i, spatial frequency is denoted by n_i and phase angle is φ. One may generate a harmonic signal through mean square value

$$\psi_x^2 = \frac{A_i^2}{2} \tag{46}$$

Therefore,

$$G_d(n_i) = \frac{\psi_x^2(n_i)}{\Delta n} = \frac{A_i^2}{2 \cdot \Delta n} \tag{47}$$

It has been shown in several works that the development of an artificial road profile using Eq. (45) is only possible if the PSD function of vertical displacements is well known, presuming a random phase angle φ_i following a uniform probabilistic distribution within range 0 to 2π. The artificial profile can be given as

$$\begin{aligned} h(x) &= \sum_{i=0}^{N} A_i \cos(2\pi \cdot n_i \cdot x + \phi_i) \\ &= \sum_{i=0}^{N} \sqrt{2 \cdot \Delta n \cdot G_d(i \cdot \Delta n)} \cdot A_i \cos(2\pi \cdot i \cdot x \cdot \Delta n + \phi) \end{aligned} \tag{48}$$

Using Eq. (47) in Eq. (45), a random road profile can be generated according to ISO classification by the following equation,

Table 2 ISO 8608 values of $G_d(n_0)$ and $G_d(\Omega_0)$

Road class	$G_d(n_0)$ (10^{-6} m^3)		$G_d(\Omega_0)$ (10^{-6} m^3)		Category
	Lower limit	Upper limit	Lower limit	Upper limit	
H1	–	32	–	2	New roadways with asphalt layers
H2	32	128	2	8	New roadways with concrete layers
H3	128	512	8	32	Old roadways layers which are not maintained
H4	512	2048	32	128	Roadways layer consisting if cobble stone layers or similar materials
H5	2048	8192	128	512	Very poor road condition
H6	8192	32,768	512	2048	Off-road condition
H7	32,768	131,072	2048	8192	–
H8	131,072	–	8192	–	–
	n_0 = 0.1 cycles/m		Ω_0 = 1 cycles/m		

$$h(x) = \sum_{i=0}^{N} \sqrt{\Delta n.} \cdot 2^{k} \cdot 10^{-3} \cdot \left(\frac{n_0}{i \cdot \Delta n}\right) \cos(2\pi \cdot i \cdot x \cdot \Delta n + \phi) \tag{49}$$

where x is the abscissa variable from 0 to L; Δn is $1/L$; $n_{\max}$ is taken as $1/B$; N is $\frac{^{n}\max}{\Delta n}$ or L/B; where $L=250$, $N=100$; and constant is denoted as k, depending on ISO road profile classification. It has also assumed integers augmenting from 3 to 9, which corresponds to the profiles from classes H1 to H8 (as shown in Table 3); here, k is assumed to take the value 3 corresponding to the class H1 road profile and $G_d(n_0)$ is taken to be 32, where n_0 is 0.1 cycles/m and φ_i is the random phase angle following an uniform probabilistic distribution within range 0 to 2π. In this work, four road conditions (H1-H4) are considered, which is shown in Figs. 4, 5, 6 and 7.

The simulation of different road categories is obtained by MATLAB/Simulink of the previously discussed ISO 8608 random input. This road profiles are simulated for five different speeds, viz. 40 kmph, 60 kmph, 80 kmph, 90 kmph and 100 kmph. Figure 4 shows H1 road condition, where unevenness of the random-type road with maximum magnitude is 0.03 m in an upward direction at 40 km/h and − .035 m in a downward direction at 100 km/h. Similarly, H2, H3 and H4 road categories have a maximum magnitude 0.06 m, 0.12 m and 0.24 m, respectively, in an upward direction at 40 km/h and − 0.65 m, − 0.12 m and − 0.24 m, in a downward direction at 100 km/h.

Table 3 k values for ISO road roughness classification

Road class		k
Lower limit	Upper limit	
H1	H2	3
H2	H3	4
H3	H4	5
H4	H5	6
H5	H6	7
H6	H7	8
H7	H8	9

5 Results and Discussion

The model is exhibited first on sine wave input from start to end and runs for 20 s with zero initial conditions. The amplitude of sine wave is 0.01 m, and the input frequency is taken 50 Hz. In Fig. 8, the magnitude of the vertical acceleration is 0.8 m/s^2 in un-damped condition, whereas acceleration amplitude has been reduced to 0.7 m/s^2 in damped condition. Thus, the magnitude of vibration has been reduced from 12 to 15% due to the impact of structural damping of the vehicle chassis. Similarly, in Fig. 9, the amplitude of pitching acceleration has been reduced up to 20% due to the influence of structural damping. However, frequencies in both conditions have almost similar values. The dead load on the center of chassis has been taken around 500 N, which lies in the downward direction.

The RMS acceleration responses of truck chassis at the first three modes at sine wave condition are shown in Fig. 10a–c. In these figures, the un-damped condition of the beam is superimposed over damped condition. The frequencies of the first three modes are 34.4 Hz, 86.89 Hz and 174.8 Hz, respectively. Figure 10a–c shows that the acceleration magnitude is continuously reduced, whereas maximum acceleration is found at the first mode, and minimum

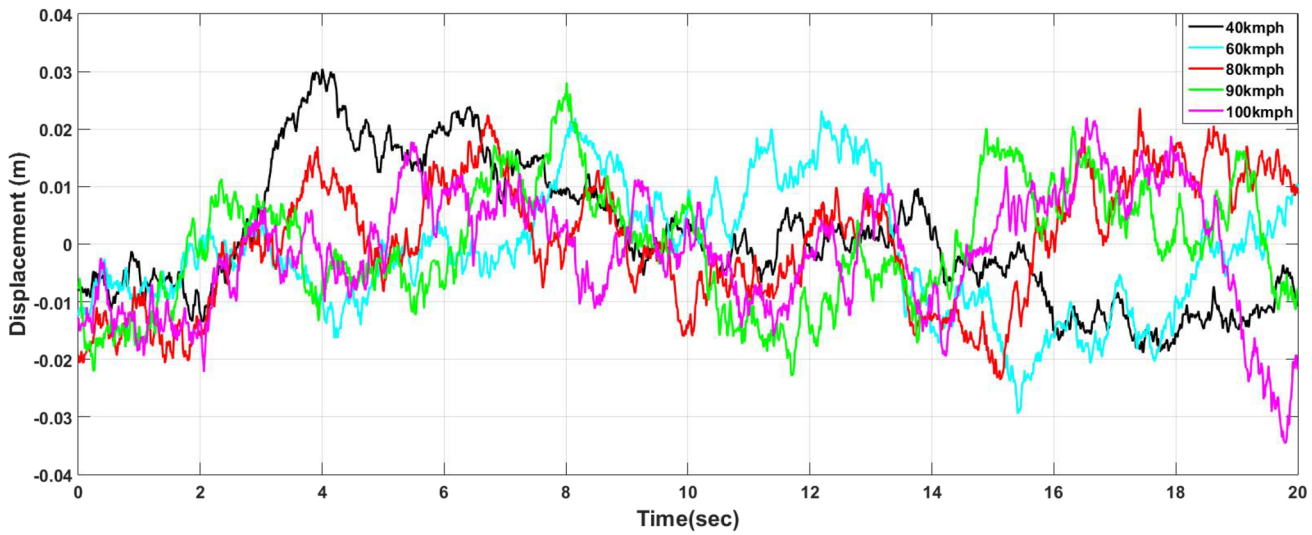

Fig. 4 Random road profile of H1 road category at 40 kmph, 60 kmph, 80 kmph, 90 kmph and 100 kmph

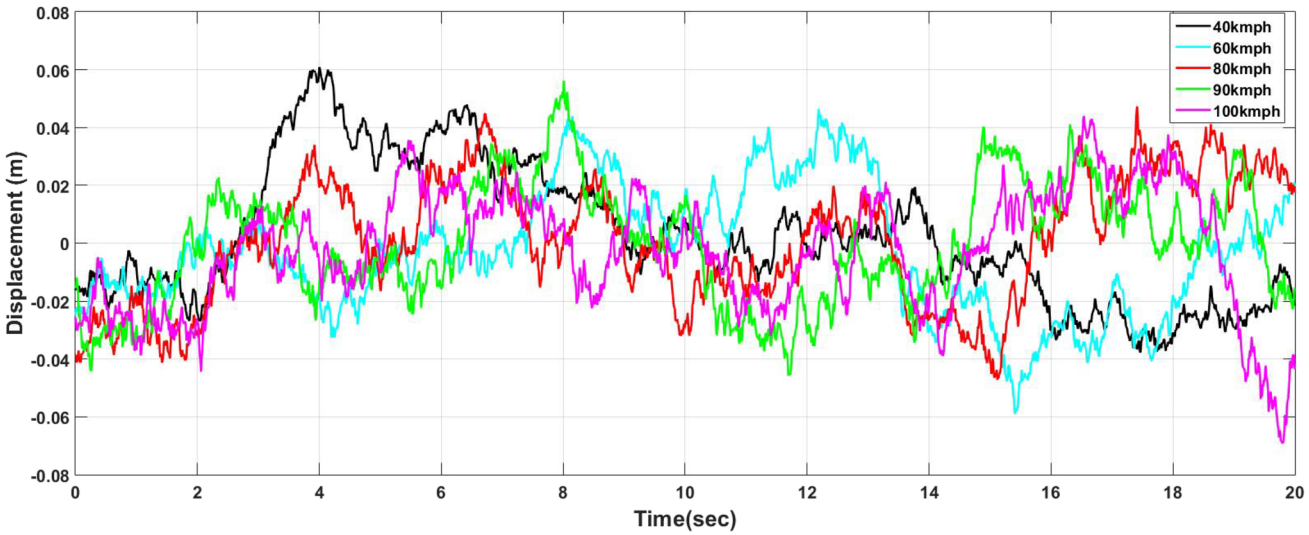

Fig. 5 Random road profile of H2 road category at 40 kmph, 60 kmph, 80 kmph, 90 kmph and 100 kmph

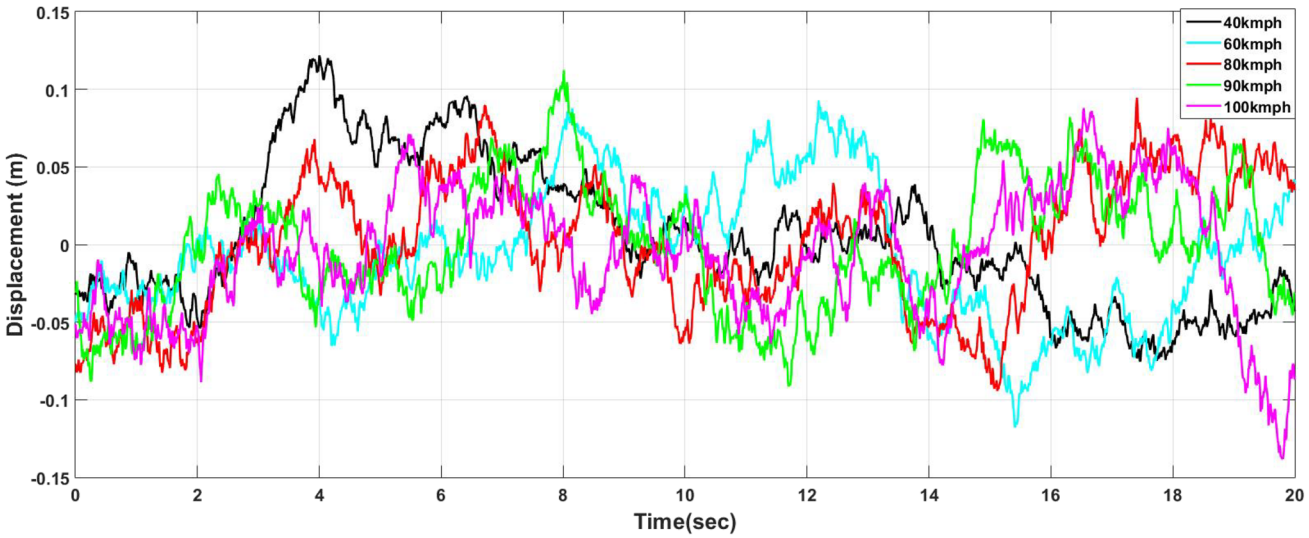

Fig. 6 Random road profile of H3 road category at 40 kmph, 60 kmph, 80 kmph, 90 kmph and 100 kmph

acceleration is in the third mode. The influence of internal damping is presented in terms of RMS acceleration response, whereas the amplitude has reduced due to the effect of internal damping at the same frequency.

The ride comfort analysis may be evaluated through RMS acceleration of the vehicle chassis. Figures 11, 12, 13 and 14 present the RMS acceleration response of the truck CG for four different classes of roads (H1–H4) as prescribed by ISO 8608. The H1 is the best class, and H4 represents the worst road class in these four classes. The model is simulated for each road class at different speeds ranging from 40 to 100 kmph with and without consideration of the internal damping of the chassis. Figures 11, 12, 13 and 14 show that the magnitude of vertical acceleration increases with vehicle speed and with road class. Figure 11a demonstrates the truck response neglecting the chassis damping, where maximum RMS acceleration magnitude is observed as 0.65 m/s^2 at 100 km/h and 0.25 m/s^2 at 40 km/h on H1 class road. This peak acceleration magnitude gets reduced up to 0.58 m/s^2 at 100 km/h and 0.22 m/s^2 at 40 km/h with due consideration to chassis structural damping, as shown in Fig. 11b. A similar kind of result has been noticed in other plots shown in Figs. 12, 13 and 14. Thus, it is evident from the above results that internal structural damping of the base structure of heavy vehicle plays an important role

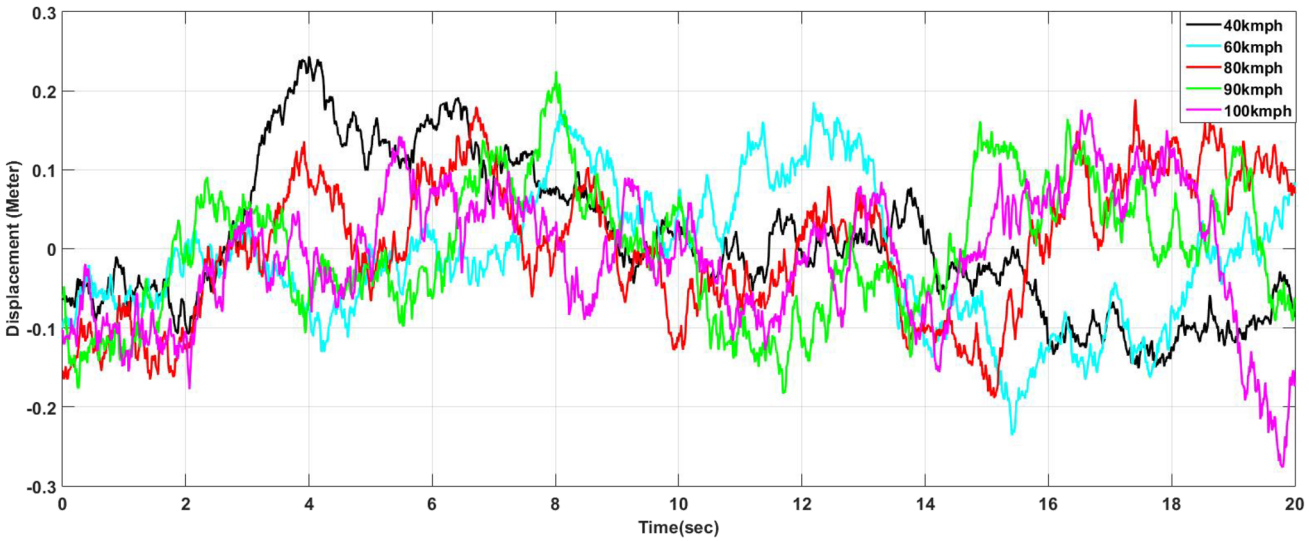

Fig. 7 Random road profile of H4 road category at 40 kmph, 60 kmph, 80 kmph, 90 kmph and 100 kmph

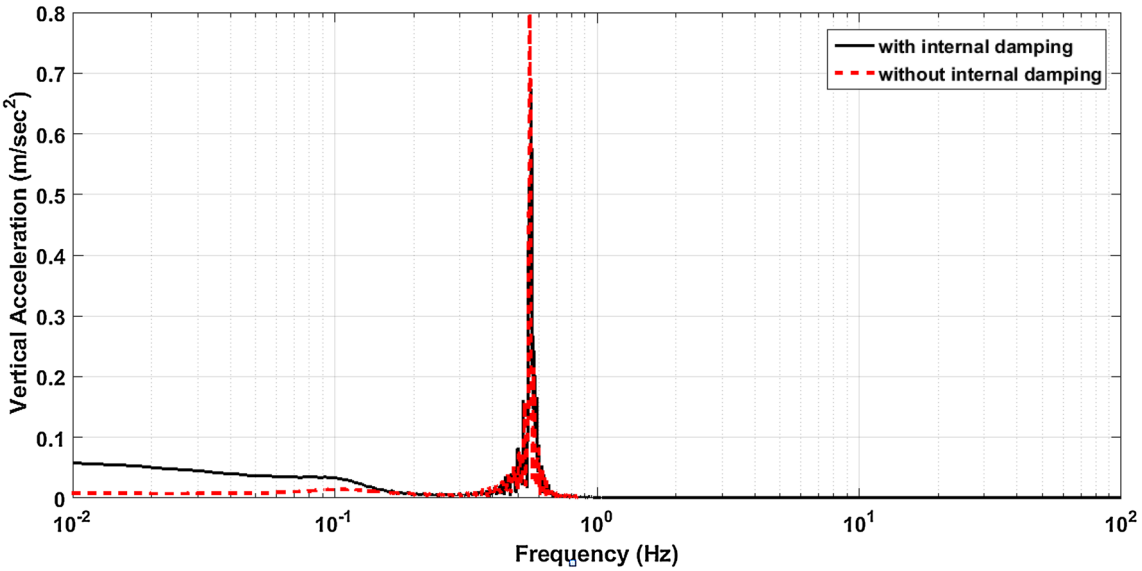

Fig. 8 Vertical response of vertical acceleration of chassis at steady-state input

and it needs to be included in the dynamical model of the vehicle to get the true dynamic behavior of the vehicle.

It has been observed that from the RMS curves that the H1 road condition is perfect for driving the vehicle for long duration, whereas it is not advisable to drive vehicles for long duration on H4 road condition. Indian roads lie between H2 and H3 conditions. So, a driver can comfortably drive the given vehicle at 60–80 km/h in single stretch without a break.

6 Conclusions

Numerous models have been constructed for the heavy vehicle system, but most of the models are developed with the lumping process. In this work, an analytical framework for truck chassis has been developed through classical mechanics and through extended Lagrangian approach. The following conclusion has been drawn from present research work:

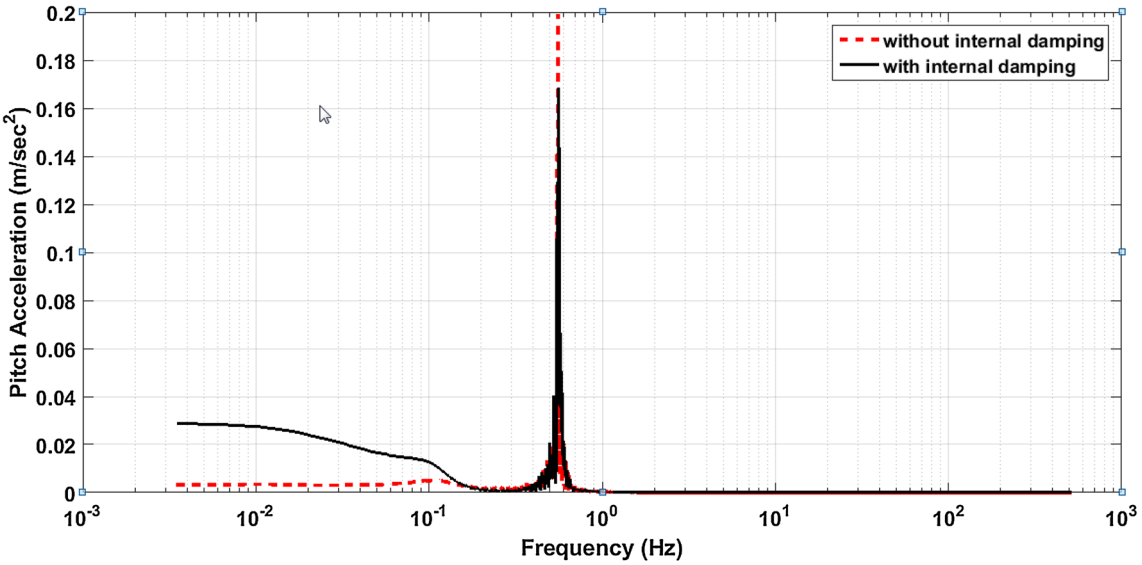

Fig. 9 Response of pitch acceleration of chassis at steady-state input

- In the classical mechanics approach, the idea of lumped–distributed modeling has been explored within the framework of bond graphs.
- The Lagrange variation of truck chassis, including flexural behavior has been constructed, where it was integrated with lumped suspension system. However, the structural damping effects were also involved in terms of fifth-order partial differential term in generalized equation of motion. The detailed derivation for fifth-order differential term is presented in "Appendix 1."
- The integrated bond graph model of flexural beam was the extended form of the analytical model. Results have been presented under the two types of road conditions, i.e., sine wave input and random road input. In sine wave road conditions, the vertical response of flexural beam is reduced up to 12–15% and pitch response of beam is reduced up to 20% due to the structural damping effect. In random road conditions, four types of road category (H1, H2, H3, H4) have been used at four different speeds (40 kmph, 60 kmph, 80 kmph and 100 kmph).
- It is depicted from the result that maximum acceleration at maximum speed (100 kmph) of chassis has been increased up to 0.5 m/s^2 in H1–H2 conditions, 1 m/s^2 in H2–H3 conditions and 2.25 m/s^2 in H3–H4 conditions. Similarly, the solution has been extended for structural or internal damping, whereas maximum acceleration at maximum speed has been reduced up to 10%, 5%, 7% and 5% (approx.) in H1, H2, H3 and H4 road conditions, respectively.

Appendix 1

This appendix gives a brief introduction to the variational formulation of dynamics of continuous systems. Consider for simplicity a one-dimensional continuous system with the field variable $w(x, t)$ which uniquely represents the configuration of the system at any time t. In the course of temporal evolution of the system, let the configurations at two time instants $t = t_1$ and $t = t_2$ be recorded as, respectively, $w(x, t_1)$ and $w(x, t_2)$. The actual path is that any infinitesimal variation over that path should leave the value of I unchanged (Hagedorn and DasGupta 2007). Now the action integral may be expressed as

$$I = \int_{t_0}^{t_1} \int_{x_0}^{x_1} \delta L(\ldots)\, \mathrm{d}t\mathrm{d}x \tag{50}$$

Using the extremization condition of Eq. (50), one may obtain

$$\int_{t_0}^{t_1} \int_{x_0}^{x_1} \delta \hat{L}\left(w, w', \dot{w}, w'', t\right) \mathrm{d}t\mathrm{d}x = 0 \tag{51}$$

One may write Lagrangian density variation,

$$\delta \hat{L} = \frac{\partial \hat{L}}{\partial w}\delta w + \frac{\partial \hat{L}}{\partial \dot{w}}\delta \dot{w} + \frac{\partial \hat{L}}{\partial w'}\delta w' + \frac{\partial \hat{L}}{\partial w''}\delta w'' \tag{52}$$

Introducing Eqs. (51) and (52), one may have

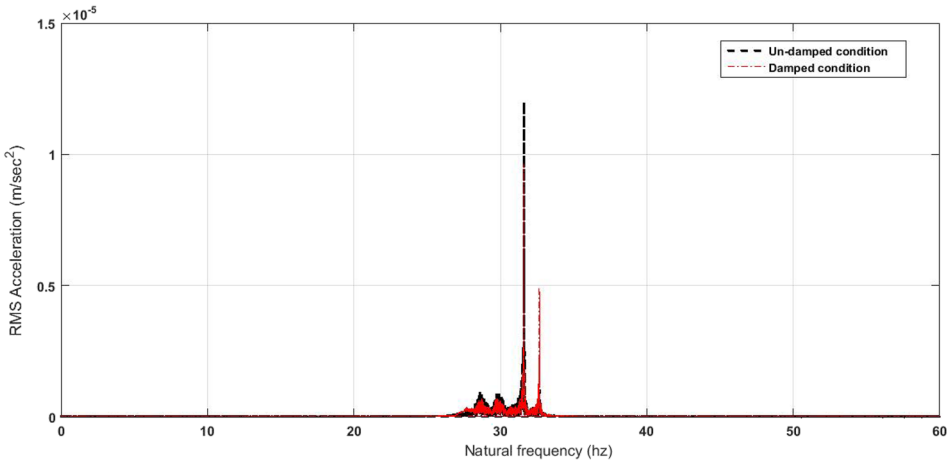
×10^-5
Un-damped condition
Damped condition
RMS Acceleration (m/sec^2)
Natural frequency (hz)

(a)

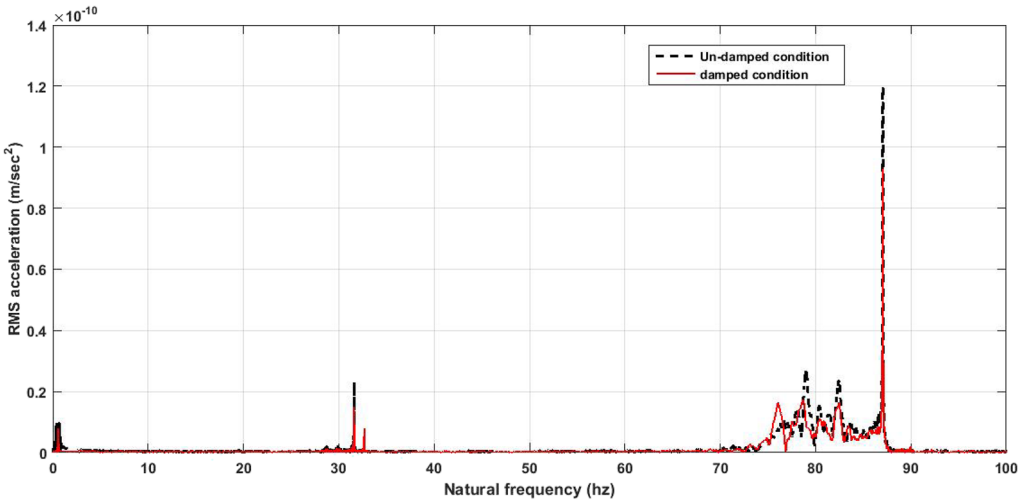
×10^-10
Un-damped condition
damped condition
RMS acceleration (m/sec^2)
Natural frequency (hz)

(b)

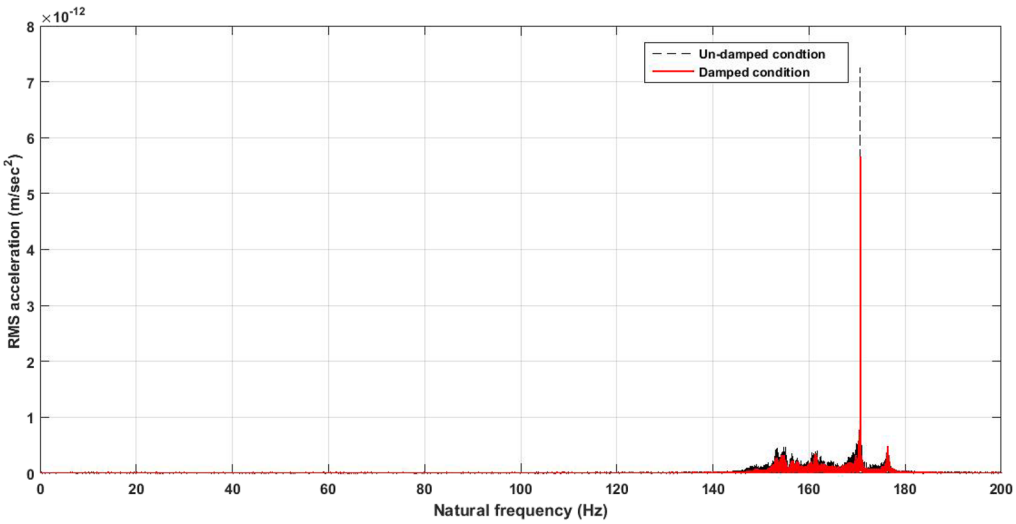
×10^-12
Un-damped condtion
Damped condition
RMS acceleration (m/sec^2)
Natural frequency (Hz)

(c)

◂**Fig. 10** RMS acceleration response of different modes of chassis under sine wave condition: **a** first mode = 34.4 Hz; **b** second mode = 86.89 Hz; **c** third mode frequency = 174.8 Hz

$$\int_{t_0}^{t_1}\int_{x_0}^{x_1}\left[\frac{\partial\hat{L}}{\partial w}\delta w+\frac{\partial\hat{L}}{\partial\dot{w}}\delta\dot{w}+\frac{\partial\hat{L}}{\partial w'}\delta w'+\frac{\partial\hat{L}}{\partial w''}\delta w''\right]\mathrm{d}t\mathrm{d}x=0 \tag{53}$$

The next step is to transform the integrand in Eq. (52) into one containing only δw, i.e., one that is free of $\delta\dot{w},\delta w',\delta w'',\delta\dot{w}'$. This can be accomplished by integration by parts, with respect to both space and time.

$$\begin{aligned}&\int_0^l\frac{\partial\hat{L}}{\partial w}\delta w\Big|_{t_1}^{t_2}\mathrm{d}x+\int_{t_0}^{t_1}\left[\frac{\partial\hat{L}}{\partial w''}\delta w''+\left\{\frac{\partial\hat{L}}{\partial w'}-\frac{\partial}{\partial x}\left(\frac{\partial\hat{L}}{\partial w''}\right)\right\}\delta w\right]\Big|_0^l\mathrm{d}t\\&+\int_{t_0}^{t_1}\int_{x_0}^{x_1}\left[\frac{\partial\hat{L}}{\partial w}-\frac{\partial}{\partial t}\left(\frac{\partial\hat{L}}{\partial\dot{w}}\right)-\frac{\partial}{\partial x}\left(\frac{\partial\hat{L}}{\partial w'}\right)+\frac{\partial^2}{\partial x^2}\left(\frac{\partial\hat{L}}{\partial w''}\right)+\frac{\partial^2}{\partial x\partial t}\left(\frac{\partial\hat{L}}{\partial\dot{w}'}\right)\right]\delta w\,\mathrm{d}t\mathrm{d}x=0\end{aligned} \tag{54}$$

But the vertical displacement δw is arbitrary by definition, which implies that it can be assigned values at will provide these values are compatible with the system constraint, such as geometric conditions at the end points. Let $\delta w=\delta w'=0$ at $x=0$ and $x=l$. One may conclude that Eq. (54) can be satisfied for all values of δw in the open domain $0<x<l$.

Thus,

$$\frac{\partial\hat{L}}{\partial w}-\frac{\partial}{\partial t}\left(\frac{\partial\hat{L}}{\partial\dot{w}}\right)-\frac{\mathrm{d}}{\mathrm{d}x}\left(\frac{\partial\hat{L}}{\partial w'}\right)+\frac{\partial^2}{\partial x^2}\left(\frac{\partial\hat{L}}{\partial w''}\right)+\frac{\partial^2}{\partial x\partial t}\left(\frac{\partial\hat{L}}{\partial\dot{w}'}\right)=0 \tag{55}$$

Equation (55) represents the *Lagrange differential equation of motion* for this continuous system and must be satisfied at every point of open domain $0<x<l$.

$$\frac{\partial\hat{L}}{\partial w''}\equiv 0\quad\text{or}\quad\delta w|_{x=0}\equiv 0 \tag{56a}$$

$$\frac{\partial\hat{L}}{\partial w''}\Big|_{x=l}\equiv 0\quad\text{or}\quad\delta w|_{x=l}\equiv 0 \tag{56b}$$

$$\frac{\partial\hat{L}}{\partial w'}-\frac{\mathrm{d}}{\mathrm{d}x}\left(\frac{\partial\hat{L}}{\partial w''}\right)\Big|_{x=0}=0\quad\text{or}\quad\delta w|_{x=0}\equiv 0 \tag{57a}$$

$$\frac{\partial\hat{L}}{\partial w'}-\frac{d}{dx}\left(\frac{\partial\hat{L}}{\partial w''}\right)\Big|_{x=l}=0\quad\text{or}\quad\delta w|_{x=l}\equiv 0 \tag{57b}$$

Equations (56–57) are known as the boundary conditions and only two boundary conditions must be satisfied at either end, one from condition Eq. (56) and other from Eq. (57), which shows that clearly the selection is not arbitrary, but it must reflect physical conditions at two ends.

Appendix 2

In this formulation, the vertical translation of a uniform free–free beam is considered. If the internal damping of the material is involved in the system, then the strain displacement relationship or Hook's law equation can be written as Karnopp et al. (2012) and Hagedorn and DasGupta (2007).

$$\sigma(x,t)=E\varepsilon(x,t)+\mu_I\varepsilon(x,t) \tag{58}$$

The strain displacement relation at any height from the plane of the neutral fibers can be written as

$$\varepsilon(x,t)=\frac{zw''(x,t)}{\left[1+w'^2(x,t)\right]^{\frac{3}{2}}}\approx -zw''(x,t)\quad(\text{Assuming } w'<<1) \tag{59}$$

The bending moment at any section (from Fig. 15) can be written as

$$M(x,t)=-\int_{h/2}^{-h/2}z\sigma(x,t)\mathrm{d}A=-\left(E\varepsilon(x,t)+\mu_I\varepsilon(x,t)\right)\int_{h/2}^{-h/2}z^2\mathrm{d}A \tag{60}$$

$$\Rightarrow\quad-\left(EIw''(x,t)+\mu_I I\dot{w}''(x,t)\right) \tag{61}$$

where I is the moment of inertia cross section of beam about the neutral axis. The equation of the vertical force of an infinitesimal beam is

$$(\rho A\mathrm{d}x)\ddot{w}(x,t)=p(x,t)\mathrm{d}x+(V+\mathrm{d}V)\cos(\psi+\mathrm{d}\psi)-V\cos\psi$$

or

$$pA\ddot{w}(x,t)=p(x,t)+V' \tag{62}$$

The rotational dynamics of infinitesimal beam may be written as

$$(\rho I\mathrm{d}x)\ddot{\psi}=(M+\mathrm{d}M)-M(V+\mathrm{d}V)\frac{\mathrm{d}x}{2}+V\frac{\mathrm{d}x}{2}$$

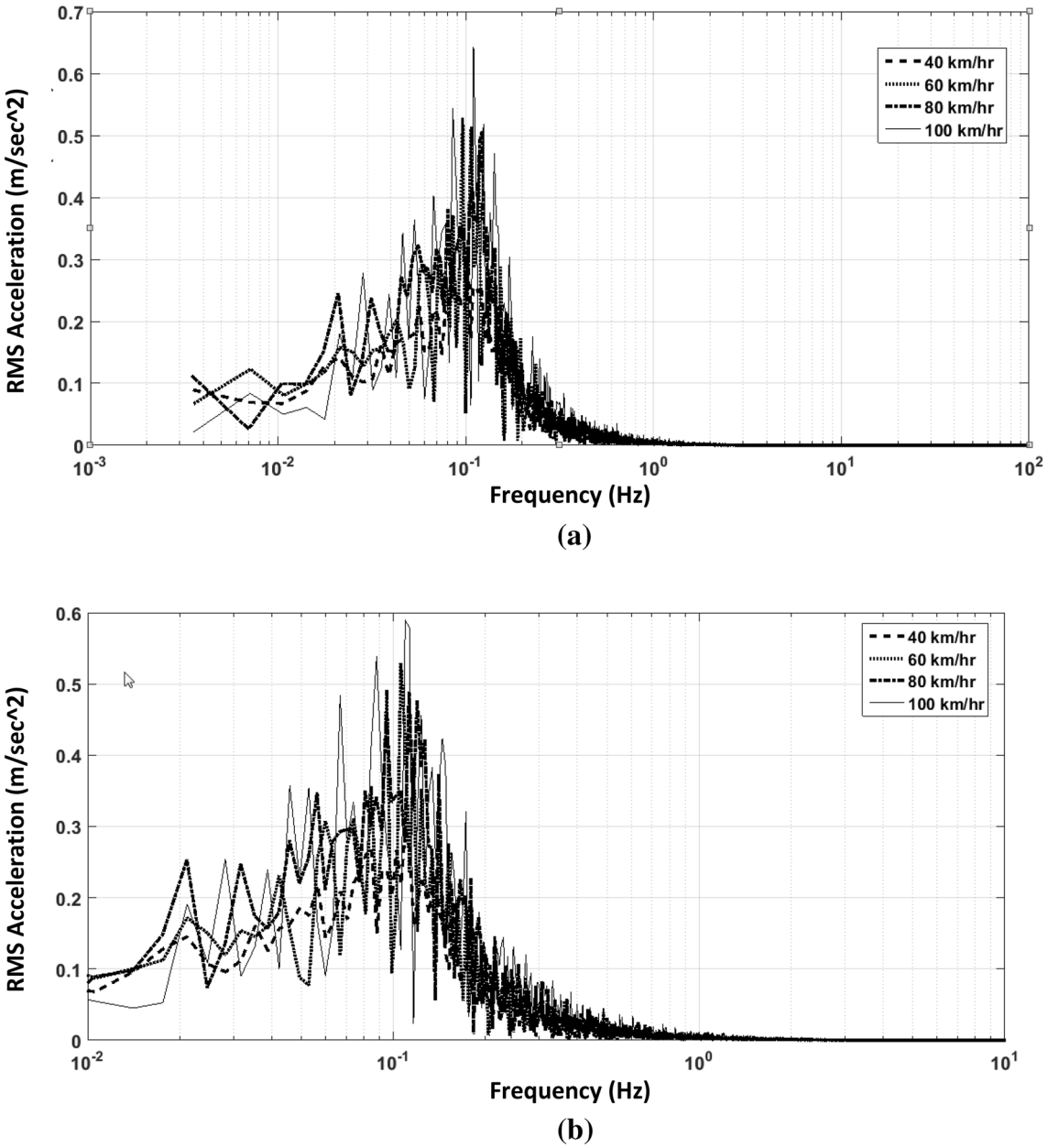

Fig. 11 **a** Response of chassis acceleration at various random road inputs in H1 road as per ISO 8608. **b** Response of chassis acceleration consideration of internal damping at different random inputs in H1 road condition as per ISO 8608

or

$$\rho I\ddot{\psi} = M' + V \tag{63}$$

One may write $\dot{\psi} = \frac{w'(x,t)}{1+w'^2(x,t)} \approx w'(x,t)$Thus, from Eqs. (62) and (63), one may have

$$\rho A\ddot{w}(x,t) - \rho I\ddot{w}''(x,t) + \mu_I I\dot{w}''''(x,t) + EIw''''(x,t) - p(x,t) = 0 \tag{64}$$

The third term of Eq. (64) represents the structural damping or internal damping of the beam.

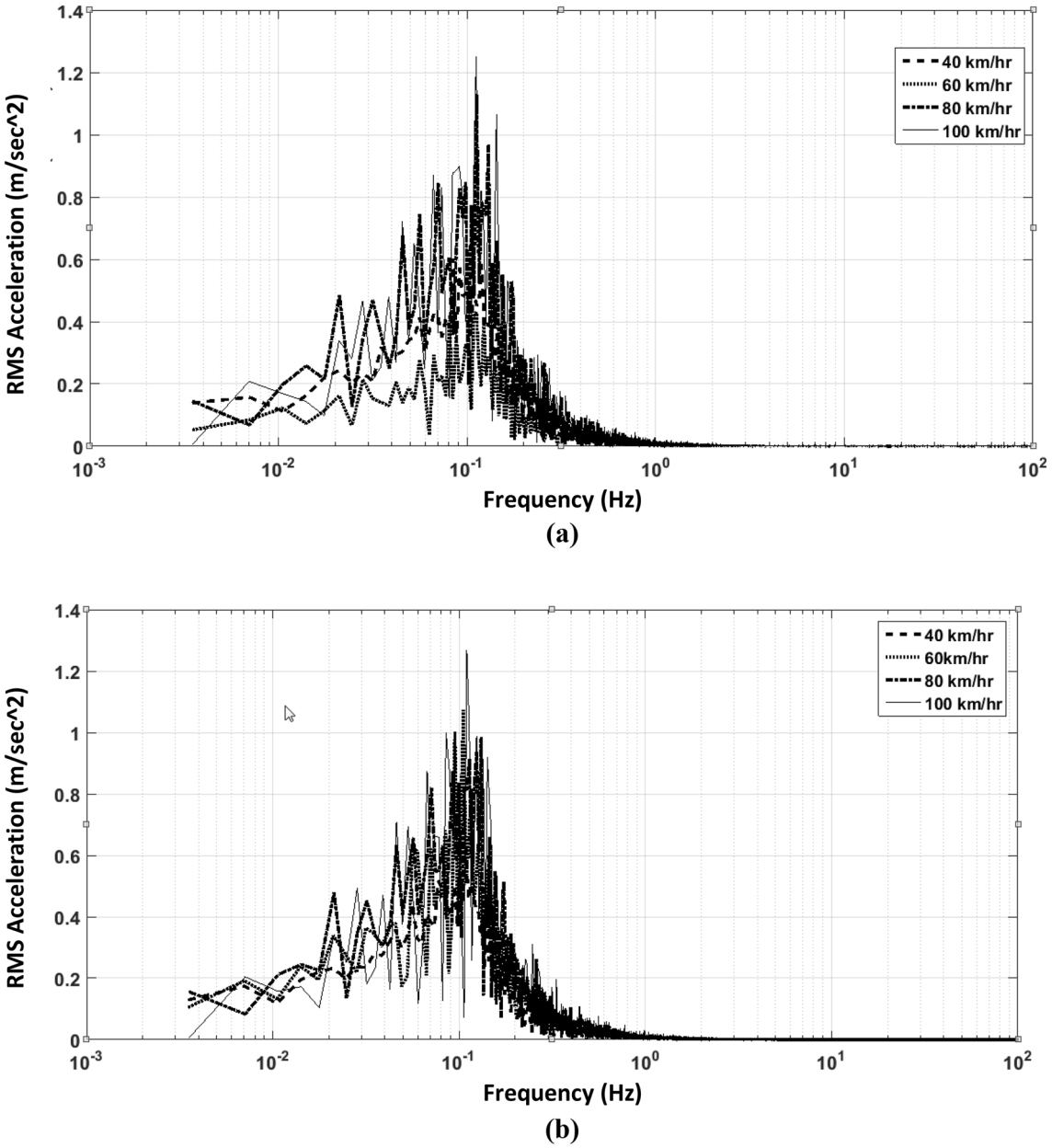

Fig. 12 **a** Response of chassis acceleration at various random road inputs in H2 road as per ISO 8608. **b** Response of chassis acceleration consideration of internal damping at different random inputs in H2 road condition as per ISO 8608

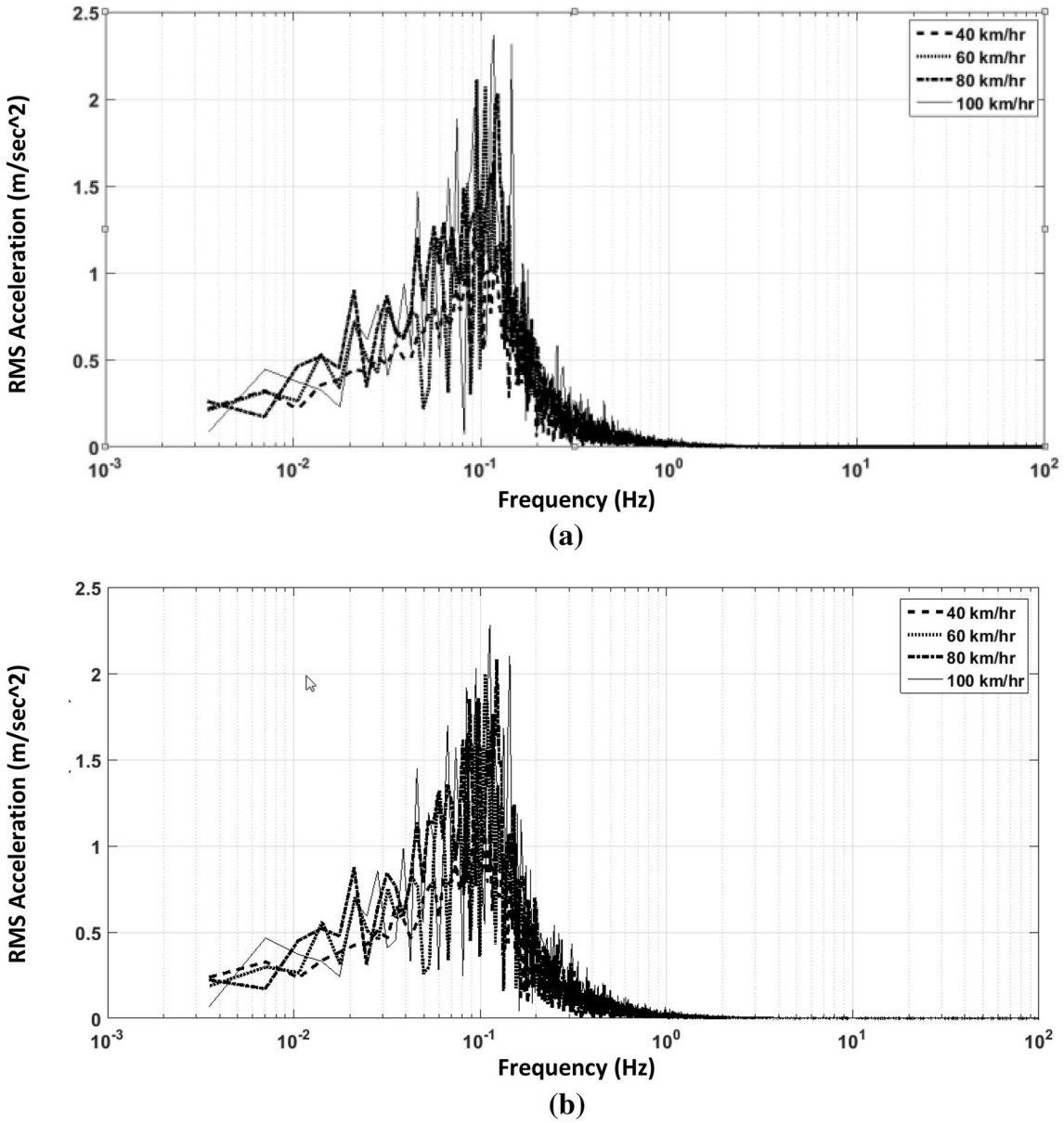

Fig. 13 **a** Response of chassis acceleration at various random road inputs in H3 road as per ISO 8608. **b** Response of chassis acceleration consideration of internal damping at different random inputs in H3 road condition as per ISO 8608

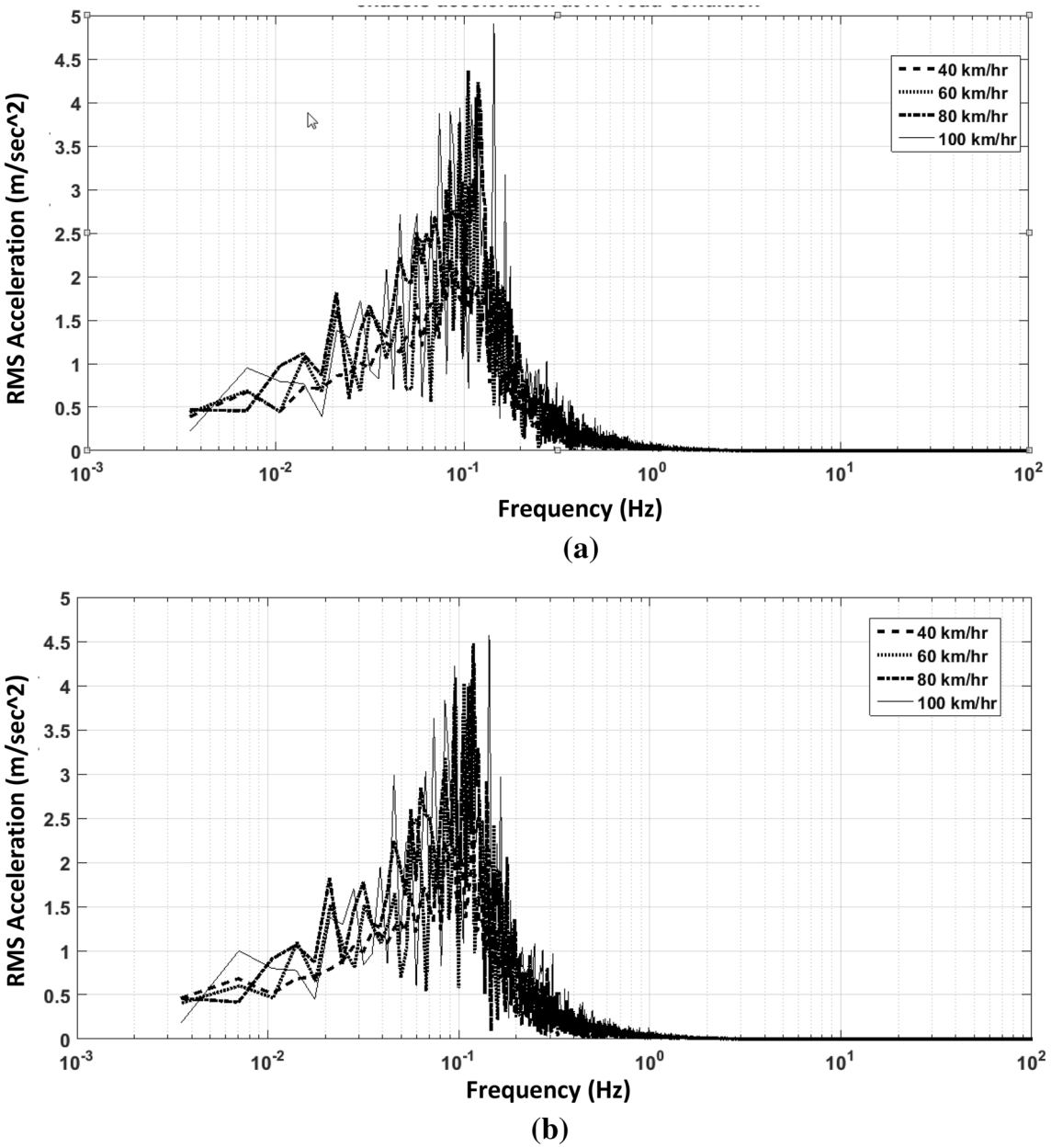

Fig. 14 **a** Response of chassis acceleration at various random road inputs in H4 road as per ISO 8608. **b** Response of chassis acceleration consideration of internal damping at different random inputs in H4 road condition as per ISO 8608

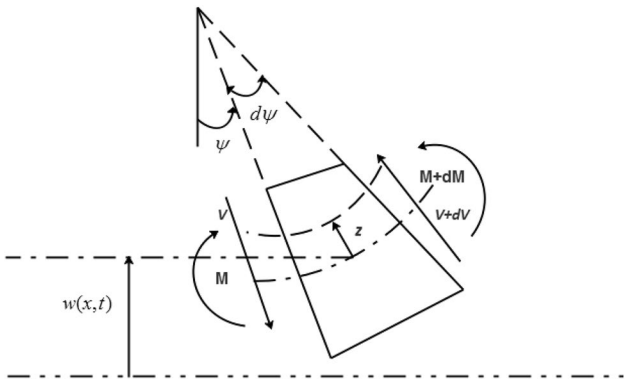

Fig. 15 Infinitesimal element of a deflected beam

References

Agostinacchio M, Ciampa D, Olita S (2014) The vibrations induced by surface irregularities in road pavements—a Matlab® approach. Eur Transp Res Rev 6(3):267–275

Gupta A, Rastogi V (2016) Effects of various road conditions on dynamic behavior of heavy road vehicle. Procedia Eng 144:1129–1137

Hagedorn P, DasGupta A (2007) Vibrations and waves in continuous mechanical systems. Wiley, New York

Hassani S (2013) Mathematical physics: a modern introduction to its foundations. Springer, Berlin

Huang CH, Zeng J (2010) Flexural vibration suppression of car body for high-speed passenger car based on constrained damping layers. J Traffic Transp Eng 10(1):36–41

Ibrahim IM (1996) Effect of frame flexibility on the ride. Vib Heavy Trucks 58(4):709–713

Karnopp DC, Margolis DL, Rosenberg RC (2012) System dynamics: modeling, simulation, and control of mechatronic systems. Wiley, New York

Kim JH, Yim HJ (1994) Influence of chassis flexibility on dynamic behavior of engine mount systems. SAE Paper, 942269

Kumar V, Rastogi V, Pathak P (2017) Simulation for whole-body vibration to assess ride comfort of a low–medium speed railway vehicle. Simulation 93(3):225–236

Margolis D, Edeal D (1989) Modeling and control of large flexible frame vehicles using bond graphs SAE Paper 892488. Society of Automotive Engineers, Warrendale

Meirovitch L (1980) Computational methods in structural dynamics. Springer, Netherlands

Mukherjee A, Karmakar R (2000) Modelling and simulation of engineering system through bond graph, Narosa Publishing House, New Delhi, reprinted by CRC Press for North America and by Alpha Science for Europe

Mukherjee A, Samantaray AK (2006) SYMBOLS-Shakti user's manual. High-Tech Consultants, STEP Indian Institute of Technology, Kharagpur

Rideout DG (2012) Simulating coupled longitudinal, pitch and bounce dynamics of trucks with flexible frames. Mod Mech Eng 2(4):176–189

Rideout D, Khan TM (2010) Flexible truck modelling and investigation of coupling between rigid and flexible dynamics. In: Proceeding of the ICBGM 2010, Orlando, USA

Tomioka T, Takigami T, Suzuki Y (2006) Numerical analysis of three-dimensional flexural vibration of railway vehicle car body. Veh Syst Dyn 44(Supp-1):272–285

Tomioka T, Takigami T, Aida K (2017) Experimental investigations on the damping effect due to passengers on flexural vibrations of railway vehicle car body and basic studies on the mimicry of the effect with simple substitution. Veh Syst Dyn 55(7):995–1011

Tomioko T, Takigami T (2015) Experimental and numerical study on the effect due to passengers on flexural vibrations in railway vehicle car bodies. J Sound Vib 343:1–19

Zhou J, Goodall A, Ren L, Zhang H (2009) Influences of car body vertical flexibility on ride quality of passenger railway vehicles. F J Rail and Rapid Transit 2009:223